
Advanced structure methodologies for next-generation ground vehicles, Part 1: Basic theories

C. Pierre*, N. Vlahopoulos*, Z.D. Ma*,
M.P. Castanier*, S.-Y. Lee*, A. Wang*,
K.K. Choi[†], N.H. Kim[†] and J. Dong[†]

*University of Michigan, Ann Arbor, MI 48109 USA

[†]University of Iowa, 2222 Old Hwy 218 S, Iowa City IA 52242-1602, USA

Corresponding author Z.D. Ma. E-mail: mazd@umich.edu

Abstract: One of the major objectives of the Automotive Research Center (a US Army TACOM Center of Excellence for the modelling and simulation of ground vehicles at the University of Michigan) is to develop new methodologies for advanced structures and materials for next-generation ground vehicles. Several major developments in this area are detailed in this paper. First, an advanced topology optimisation technique is presented, which provides a tool for laying out new, conceptually advanced designs for vehicle structures, or substructures, to achieve the lower weight and higher performance requirements for next-generation ground vehicles. Second, a 'sizing' design optimisation process is presented for detailed design changes in order to improve the vibrant-acoustic response of a complex vehicle structure. This process incorporates efficient analysis and sensitivity analysis capabilities for vibro-acoustic systems. In addition, a component-based technique is presented for generating reduced-order models of a vehicle structure in order to lower the computational costs of vibration analysis. This technique is also extended to analysing vibration transmission in a complex vehicle structural system to determine the power flow among components and the effect of parameter uncertainties. Finally, an energy boundary element analysis method is presented for efficient and accurate high-frequency noise analysis, which extends the capability for predicting the acoustic field around the vehicle due to various sources.

Keywords: advanced materials, advanced structures, ground vehicles, topology optimisation.

Reference to this paper should be made as follows: Pierre, C., Vlahopoulos, N., Ma, Z.D., Castanier, M.P., Lee, S.-Y., Wang, A., Choi, K.K., Kim, N.H. and Dong, J. (2004) 'Advanced structure methodologies for next-generation ground vehicles, Part 1: Basic theories', *Int. J. Heavy Vehicle Systems*, Vol. 11, Nos. 3/4, pp. 257–281.

1 Introduction

The US Army Tank-Automotive & Armaments Command (TACOM) has two major programs, Future Combat Systems (FCS) and Improved Materials and Powertrain Architectures for 21st Century Trucks (IMPACT). The goal of the FCS program is to develop Army combat systems with significantly improved deployability, mobility, and survivability. These systems are required to have Abrams-tank-equivalent (or better) lethality and survivability in a smaller, lighter package, and they must be able to be deployed in less time than current forces. The systems must fit within the cargo volume of a C-130 aircraft and weigh no more than 20 tons. Considering that the current M1 Abrams tank weighs about 70 tons, the FCS program demands revolutionary concepts in vehicle design as well as a means to optimally design the vehicle structures in order to make use of every pound of material. New techniques have to be developed to fit these needs, which include modularisation of the subsystem designs, optimisation techniques for both vehicle concept designs and detailed subsystem designs, and advanced prediction capabilities for vehicle dynamics, vibration, noise, and durability.

The primary mission of the IMPACT program is to increase significantly the fuel economy of light, medium, and heavy trucks, while at the same time improving vehicle performance and reducing carbon-dioxide emissions. The Army's long-term goal is a 75% reduction in fuel requirements for a deployed force. These improvements need to be achieved while maintaining current levels of cost and safety. Trucks provide the logistical backbone to the Army, while fuel constitutes 70% of bulk tonnage needed to sustain a military force on the battlefield. Trucks are also vital to the USA; they account for over 75% of the nation's freight business and burn more fuel than cars. To achieve the goals defined in the IMPACT program, techniques are needed for laying out new concepts of vehicle design and to optimise vehicle systems.

The Automotive Research Center (ARC) is a US Army TACOM Center of Excellence for Modelling and Simulation of Ground Vehicles at the University of Michigan. One of the major objectives of the ARC is to develop new methodologies for advanced structures and materials for next-generation ground vehicles. This includes the development of new models, analysis techniques, design sensitivity analysis methods, and optimisation techniques for lightweight and high-performance structures that minimise vibration and noise and maximise the durability and fatigue life of advanced vehicle systems. Several key research issues are listed below:

- 1 efficient modelling techniques for vehicle dynamics, vibration, radiated noise, and acoustic signature
- 2 predictions of noise, vibration, and harshness (NVH) across a wide frequency spectrum – from low- to mid- to high-frequency ranges
- 3 analysis and sensitivity analysis capabilities for an emerging class of lightweight vehicle body structures (e.g. hybrid vehicles), which are likely to suffer from vibration problems
- 4 new simulation and modelling tools to enable durability analyses and design
- 5 advanced optimal design techniques for developing new concepts of vehicle structure designs and for optimising vehicle designs
- 6 integration of models in a distributed, flexible design environment.

In this two-part study, several major research developments related to these topics are presented. In this paper, the basic theories and formulations are covered. In the companion paper, applications to example vehicle structures are shown.

2 Major developments

To address the issues stated in the previous section, several developments have been carried out, four of which will be detailed in this paper. First, an advanced topology optimisation technique is presented for generating concept designs of new vehicle structures. This technique provides capabilities for laying out novel, conceptually advanced designs for vehicle structures or substructures to achieve the goals of reduced weight and increased performance. Second, a ‘sizing’ design optimisation process is described for achieving detailed design changes in order to improve the vibration and noise response of a complex vehicle structure. This development includes efficient prediction and sensitivity analysis capabilities for vibrant-acoustic systems. Third, a component-based reduced order modelling (ROM) technique is presented that allows efficient vibration analysis. This technique is also extended for analysing vibration transmission in a vehicle structural system in order to determine the power flow between components and to predict the effect of parameter uncertainties. Fourth, an energy boundary element analysis (EBEA) method for high-frequency noise analysis is covered. This EBEA method extends the capabilities for predicting the acoustic field around the vehicle due to various noise sources.

2.1 Topology optimisation for innovative concept design of vehicle structure

A breakthrough technique for the topology optimisation of structural systems was introduced in 1988 (Bendsøe, and Kikuchi, 1988), and it is known as the *homogenisation design method*. In this method, the topology optimisation problem for a structure is transformed into an equivalent problem of optimum material distribution by considering both the ‘microstructure’ and the ‘macrostructure’ in the design domain. The topology optimisation technique overcomes the barrier posed by the concept design process of a structure and makes it possible to obtain a truly optimum design that is independent of the initial guess for the structural topology. This technique has been applied to many different problems, including both structural designs and material designs. In the current research, the topology optimisation technique is extended to optimise a chassis frame structure in a truck system. A multi-domain, multi-step topology optimisation technique is developed, which allows the designer to control better the material distribution in the optimisation process and to improve significantly manufacturability of the final design. From an initial study of the truck system, it was determined the peak resonant noise inside the cabin of the truck was due to an in-plane vibration mode of the chassis frame. It is shown that the chassis frame design will have the major influence on the peak noise predicted. To demonstrate the feasibility of the topology optimisation technique, a two-dimensional design problem is considered for laying out conceptually novel designs for achieving desired in-plane eigenmodes that result in reduced vibration and noise.

2.2 *NVH design sensitivity analysis and optimisation using a finite element-boundary element approach*

The objective of this research initiative is to provide design sensitivity analysis and optimisation capabilities for NVH problems of wide frequency range. The NVH design sensitivity analysis tool will enable the design of vehicles with better ride quality, and it can be used to ensure the ride quality when the vehicle weight is minimised in order to achieve the fuel efficiency. In military applications, controlling NVH is necessary for combat ability of the personnel inside the vehicle and for protecting onboard instruments from harsh off-road conditions. This may also provide a means for managing the acoustic signature of the vehicle so that it cannot be detected by the enemy.

An efficient and accurate design sensitivity analysis (DSA) method has been developed using a sequential adjoint variable approach for NVH models based on finite element analysis (FEA) and boundary element analysis (BEA). The adjoint load is obtained from the boundary element re-analysis, and the adjoint response is obtained from structural finite element re-analysis. The design variables used in the optimisation process can be a wide range of modelling parameters, including thickness of the panels that form the body structure, material properties of the structure, and many others. Sensitivities obtained for the structural-acoustic system are then utilised in an optimisation process for given objectives and constraints, which will be discussed in detail in Section 3.2. This new capability has also been extended to include a new model reduction technique, which will be detailed in the next subsection.

2.3 *Reduced order modelling technique*

A technique has been developed for generating reduced-order models (ROMs) of vibration and for predicting power flow from a finite element model of arbitrary size and complexity. This method is based on component mode synthesis, but in addition to the classical component modes, an additional set of modes, called the characteristic constraint (CC) modes, is employed. By truncating the set of CC modes, highly efficient yet accurate models of vibration and power flow can be generated for a selected frequency band, including the mid-frequency range. The CC-mode-based ROM can then be integrated with the design sensitivity analysis method mentioned previously to achieve better efficiency for both sensitivity analysis and structural re-analysis in an optimal design process.

The size of the ROMs may be selected based on the frequency range of interest as well as the desired accuracy and efficiency. The ROM basis is used as a framework for analysing structural vibration, calculating power flow between components, and estimating the effect of parameter uncertainties on the vibratory response. For predicting the influence of uncertainties (e.g. manufacturing tolerances) on the system response, each modal response is expanded in a series of globally orthogonal polynomials or locally linear interpolation functions (finite elements) in the uncertain parameters, and the system equations are derived using the Galerkin method. This allows one to compute the ensemble-averaged power flow based on the ROM. The new technique provides a simulation capability for predicting vibratory response of vehicles and vehicle components, enables the prediction of the effect of parameter uncertainties, supports the assessment of vehicle noise, and supports design sensitivity analysis and optimisation of vehicle structures.

2.4 Energy boundary element analysis (EBEA) method for high-frequency analysis of acoustic field

The objective of this research initiative is to develop a new formulation for structural acoustic computations of complex vehicle structures that are comprised of stiff and flexible members that demonstrate, respectively, low and high modal overlap. Energy boundary element analysis (EBEA) constitutes a new formulation for computing high-frequency acoustic radiation. It has been utilised in evaluating the airborne noise in the vicinity of the vehicle and for making a comparison of the airborne acoustic field between a conventional and a hydraulic hybrid truck. EBEA provides a significant improvement over the popular statistical energy analysis (SEA) approach for high-frequency exterior acoustic analysis. SEA approximates an exterior domain as an assembly of several enclosed cavities and requires the definition of artificial damping and non-physical coupling loss factors between subsystems. The new EBEA formulation eliminates all these approximations. In addition, a hybrid FEA development effort (Vlahopoulos and Zhao, 1999; Hong, and Vlahopoulos, 2003) is continued for coupling conventional FEA with energy finite element analysis (EFEA). Analyses are performed using a conventional dense FEA model and a hybrid FEA approach for an assembly of plates spot-welded on a frame structure. Results from the two methods are compared successfully in the mid-frequency range.

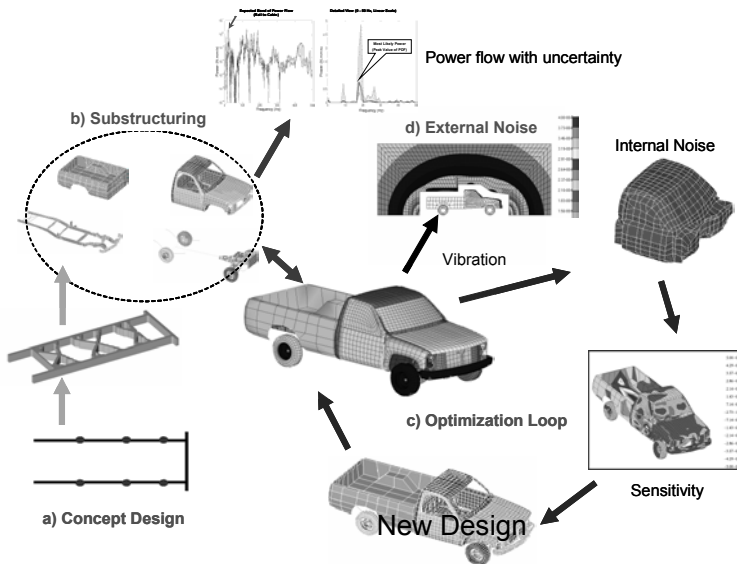


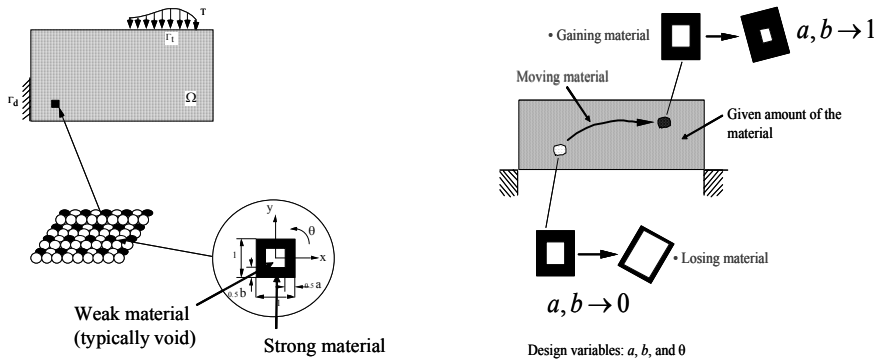
Figure 1 A case study for the new methodologies developed.

2.5 Integration of methodologies and application to a case study

Figure 1 illustrates how the methodologies described above were integrated and applied to a case study of a pick-up truck. This case study will be discussed in detail in the second part of this paper.

3 Basic theories

In this section, the basic theories are presented for the research developments described in the previous section



(a) Microstructures in a structural domain.

(b) Moving material from a region of the structural domain into another region.

Figure 2 Basic concept of the homogenisation based topology optimisation method.

3.1 Topology optimisation

A topology optimisation technique was developed by Bendsøe and Kikuchi in 1988, and it has since become known as the *homogenisation-based topology optimisation* method. The basic idea in this technique is to transform the optimal topology design problem into an equivalent Optimal Material Distribution (OMD) problem, using a composite material that has a variable microstructure (Bendsøe and Kikuchi, 1988,5). As shown in Figure 2(a), consider that the structural domain is filled with a non-homogeneous composite material with a variable microstructure. As a simplification, consider a plane-stress problem, and assume that the microstructure is formed inside an empty rectangle in a unit cell with three design variables a , b and θ . Here, a and b are the sizes of the microstructure, and θ is the orientation of the microstructure. In the optimisation process, the microstructure can vary between 'empty' and 'solid' using the design variables a and b , and it can be rotated using the orientation variable θ . The microstructure becomes a complete void when $a = b = 0$, and a complete solid when $a = b = 1$. Therefore, if one assumes that the total amount of the material – which is prescribed for the design problem at hand – remains constant in the optimisation process, then the material will be moved from a region of the structural domain into another region to produce a new distribution of the material, as depicted in Figure 2(b). By moving and orienting the material so as to improve the objective function of the optimisation problem, one can finally obtain an OMD that corresponds to the optimal structure. This approach can be easily extended to deal with a three-dimensional problem.

The topology optimisation method described above has been applied to various areas, including structural design and material design. It has also been used in the design of

structures, materials, and micro-electro-mechanical system (MEMS), for achieving static stiffness, mechanical compliance, desired eigenfrequencies, reduced dynamic response, desired material properties, unusual thermo-elastic properties and other objectives (Ma, Z.-D., Kikuchi, N. and Hagiwara, I., 1993; Nishiwaki, *et al.*, 1998). Basic formulations for the *homogenisation-based topology optimisation* method can be found in (Bendsøe and Kikuchi. 1988) for a static problem and in (Ma, *et al.*, 1995) for dynamic problems.

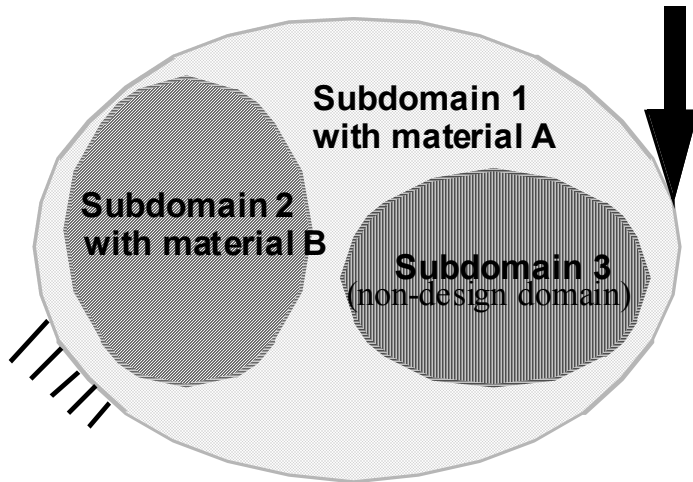


Figure 3 A multi-domain topology optimisation problem.

The topology optimisation technique developed in (Bendsøe and Kikuchi. 1988; Ma, *et al.*, 1995) has been extended to a multi-step multi-domain topology optimisation (MMTO) method (Ma, *et al.*, 2002; Wang, *et al.*, 2003). In contrast to single-domain topology optimisation, in which a given amount of the material is assigned to the entire design domain, MMTO allows the designer to assign different amounts of the material, or even different materials, to the different subdomains of the structure. For example, Figure 3 shows a structural domain divided into several subdomains, where a certain amount of the material A is distributed into Subdomain 1, and a different amount of the material B is distributed into Subdomain 2. Furthermore, Subdomain 3 is considered as a non-design domain, where the material distribution is not allowed to change at the current design stage.

In the general case, the optimisation problem of the MMTO can be written as

$$\begin{aligned}
 & \text{Minimise } f(\mathbf{X}) \\
 & \text{Subject to } h_j(\mathbf{X}) \leq 0 \quad (j = 1, 2, \dots, m) \\
 & \quad \underline{x}_j \leq x_j \leq \bar{x}_j \quad (j = 1, 2, \dots, n)
 \end{aligned} \tag{1}$$

where $f = f(\mathbf{X})$ denotes the objective function, which can be the compliance (or static

stiffness) (see, e.g. (Bendsøe and Kikuchi, 1988)), the mean eigenvalue (see (Ma et al., 1995; Ma et al., 1994; Ma et al., 1995)), the frequency response (see Ma et al., 1993), the mutual energy (Fecker et al. 1997; Kikuchi et al., 1998; Nishiwaki et al., 1998), or a combination of the objectives aforementioned, or any others; h_j denotes the j -th constraint function for the volume (or weight) of the j -th substructure in the j -th subdomain (where $j = 1, 2, \dots, m$); $\mathbf{X} = \{x_1, x_2, \dots, x_n\}^T$ denotes the vector of the design variables; and \underline{x}_j and \bar{x}_j are the lower and upper bounds of design variable x_j , respectively. Note that $f(\mathbf{X})$ in Equation (1) also needs to satisfy the state equations for the structural problem at hand. These state equations may include, for example, the static equilibrium equation, the equation that defines the free vibration eigenvalue problem, or the equation for the dynamic response.

The optimisation problem, Equation (1), usually involves a huge number of design variables, thus requiring a highly efficient optimisation algorithm. Because traditional mathematical programming methods are not practical for dealing with such a large number of design variables, optimality criteria (OC) methods (e.g. Berke and Khot, 1987) and sequential approximate optimisation (SAO) methods, such as SLP (Sequential Linear Programming), SQP (Sequential Quadratic Programming), and CONLIN (Convex Linearisation (Fleury and Braibant., 1986)), were employed for solving the problem. Ma and Kikuchi (1995) developed a general SAO (GSAO) method, which can be considered as an enhancement and generalisation of the previous OC and SAO algorithms, and which includes the aforementioned algorithms as special cases. The GSAO method is used here.

The general updating rule for the GSAO algorithm can be written as

$$x_i^{k+1} = g_i(x_i^k) \quad (i = 1, 2, \dots, n) \tag{2}$$

where x_i^k denotes the value of the design variable x_i at the previous (k -th) iteration step, x_i^{k+1} denotes the updated value of the design variable x_i at the current ($k+1$ th) step, and is a function defined by solving the following equation:

$$\bar{a}_i \operatorname{sgn}\{x_i - c_i\} |x_i - c_i|^{\xi_i - 1} + \sum_{j=1}^m \lambda_j \bar{b}_{ji} \operatorname{sgn}\{x_i - e_{ji}\} |x_i - e_{ji}|^{\zeta_{ji} - 1} = 0 \tag{3}$$

where x_i^{k+1} is the solution of Equation (3) for x_i , and \bar{a}_i^k and \bar{b}_{ji}^k are the functions of x_i^k :

$$\bar{a}_i^k = \operatorname{sgn}\{x_i^k - c_i\} |x_i^k - c_i|^{1 - \xi_i} f_{,x_i}, \quad \bar{b}_{ji}^k = \operatorname{sgn}\{x_i^k - e_{ji}\} |x_i^k - e_{ji}|^{1 - \zeta_{ji}} h_{j,x_i} \tag{4}$$

where $f_{,x_i} = \left. \frac{\partial f}{\partial x_i} \right|_{\mathbf{X}=\mathbf{X}^k}$ and $h_{j,x_i} = \left. \frac{\partial h_j}{\partial x_i} \right|_{\mathbf{X}=\mathbf{X}^k}$. Here λ_j is the so-called Lagrange multiplier (or dual variable) that is related to the j -th constraint of Equation (1); it is obtained by solving a dual problem of Equation (1) as discussed in Ma and Kikuchi

(1995). Note that ξ_i , ζ_{ji} , c_i and e_{ji} are parameters which define different updating rules for the GSAO algorithm. For instance, the GSAO updating rule 3 (which is an extension of the OC algorithm) is obtained by assuming $e_{ji} = c_i$ and $\zeta_{ji} = \zeta_i, (j = 1, 2, \dots, m)$. Then Equation (2) becomes

$$x_i^{k+1} = c_i + \text{sgn} \left\{ x_i^k - c_i \right\} \left(-\frac{q_i^k}{a_i} \right)^{\eta_i} \quad (5)$$

where

$$q_i^k = \sum_{j=1}^m \lambda_j \bar{b}_{ji}^k \quad \text{and} \quad \eta_i = \frac{1}{\xi_i - \zeta_i} \quad (6)$$

Note that the original OC algorithm (e.g. that used in (Bendsøe and Kikuchi, 1988)) is a special case of Equations (5) and (6) when $c_i = 0$ and $m = 1$. More updating rules can be obtained from the GSAO method using updating Equation (2). For instance, GSAO updating rule 1 is an extension of the CONLIN algorithm proposed by Fleury and Braibant (1986), GSAO updating rule 2 is an extension of the MMA algorithm proposed by Svanberg (1987), and GSAO updating rule 4 is an extension of the DSQP algorithm proposed by Fleury (1987).

3.2 NVH design sensitivity analysis and optimisation using FEA and BEA

Design sensitivity analysis (DSA) is an essential process in the gradient-based structural optimisation process, for example, in the optimisation process mentioned in the previous subsection. Here, a sequential structural-acoustic design sensitivity analysis method is presented in which structural and the acoustic behaviors are de-coupled. The method based on the continuum forms is briefly described. The original development work and a more detailed formulation can be found in Kim *et al.* (2002); Kim *et al.* (2001); and Choi *et al.* (1997).

First, using the continuum energy forms, the variational equation for the frequency response of a structural system can be written as:

$$j\omega d_u(\mathbf{v}, \bar{\mathbf{z}}) + \mathbf{K} \alpha_u(\mathbf{v}, \bar{\mathbf{z}}) = \ell_u(\bar{\mathbf{z}}), \quad \forall \bar{\mathbf{z}} \in Z \quad (7)$$

where ω denotes excitation frequency, ϕ is the structural damping coefficient, $j = \sqrt{-1}$, $\kappa = (1 + j\phi) / j\omega$, $d_u(\bullet, \bullet)$ is the kinetic sesqui-linear form, $\alpha_u(\bullet, \bullet)$ is the structural sesqui-linear form, and $\ell_u(\bullet)$ is the load semi-linear form. The definitions of the sesqui-linear and semi-linear forms can be found in Kim *et al.* (2002).

Then using a boundary element method (Ciskowski and Brebbia, 1991), the sound pressure at any point inside the acoustic cavity due to structural velocity field, \mathbf{v} , can be calculated as

$$b(\mathbf{x}_0; \mathbf{v}) + e(\mathbf{x}_0; \mathbf{p}_S) = \alpha p(\mathbf{x}_0) \quad (8)$$

where p is the sound pressure at any point \mathbf{x}_0 , \mathbf{p}_s is the sound pressure vector at the surface of the structural domain, $b(\mathbf{x}_0; \bullet)$ and $e(\mathbf{x}_0; \bullet)$ are linear integral forms that correspond to the BEM governing equation Kim, *et al.* (2002), constant α is equal to 1 for \mathbf{x}_0 inside the acoustic volume, 0.5 for \mathbf{x}_0 on a smooth boundary surface, and 0 for \mathbf{x}_0 outside the acoustic volume. The sound pressure \mathbf{p}_s on the structural surface can be obtained by evaluating Equation (8) on the structural surface as

$$A(\mathbf{p}_s) = B(\mathbf{v}) \tag{9}$$

where, $A(\bullet)$ and $B(\bullet)$ are the corresponding integral forms in Equation (8) evaluated at structural surface. After discretisation of Equation (8), the sound pressure inside the acoustic volume can be expressed by

$$p = (\mathbf{b} + \mathbf{B}^T \mathbf{A}^{-T} \mathbf{e})^T \quad \mathbf{v} = (\mathbf{b} + \mathbf{B}^T \boldsymbol{\eta})^T \quad \mathbf{v} = \mathbf{L}^T \mathbf{v} \tag{10}$$

where \mathbf{A} , \mathbf{B} , \mathbf{b} , \mathbf{e} are the matrices or vectors corresponding to the linear integral forms, and $\boldsymbol{\eta}$ is the so-called *first adjoint variable vector*. The first adjoint variable vector is used in calculating the acoustic response and then the *adjoint load*, and it is the solution of the following linear algebraic equation

$$\mathbf{A}^T \mathbf{h} = \mathbf{e} \tag{11}$$

Here $\boldsymbol{\eta}$ is only a function of the geometry of the acoustic cavity and properties of the sound field, and it is independent of the excitations in the system. The term \mathbf{L} ($\mathbf{L} = \mathbf{b} + \mathbf{B}^T \boldsymbol{\eta}$) in Equation (10) is the so-called *adjoint load*, since it will be used in Equation (15) as a load vector for obtaining the *second adjoint variable vector*. In addition, \mathbf{L} has an important physical meaning: each element in \mathbf{L} represents the contribution to the sound pressure of a unit velocity excitation at a corresponding structural node.

For an acoustic performance measure inside the acoustic cavity, differentiating Equations (8) and (7) with respect to a design variable α_i yields

$$\frac{\partial p}{\partial \alpha_i} = b\left(\mathbf{x}_0; \frac{\partial \mathbf{v}}{\partial \alpha_i}\right) + e\left(\mathbf{x}_0; A^{-1} \circ B\left(\frac{\partial \mathbf{v}}{\partial \alpha_i}\right)\right) \tag{12}$$

and

$$j\omega d_{\mathbf{u}}\left(\frac{\partial \mathbf{v}}{\partial \alpha_i}, \bar{\mathbf{z}}\right) + \kappa a_{\mathbf{u}}\left(\frac{\partial \mathbf{v}}{\partial \alpha_i}, \bar{\mathbf{z}}\right) = \ell^t_{\partial \mathbf{u}}(\bar{\mathbf{z}}) - j\omega d^t_{\partial \mathbf{u}}(\mathbf{v}, \bar{\mathbf{z}}) - \kappa a^t_{\partial \mathbf{u}}(\mathbf{v}, \bar{\mathbf{z}}) \quad \forall \bar{\mathbf{z}} \in Z \tag{13}$$

where $\frac{\partial p}{\partial \alpha_i}$ denotes the sensitivity of sound pressure p with respect to the design variable α_i ; $\frac{\partial \mathbf{v}}{\partial \alpha_i}$ denotes sensitivity of structural velocity field \mathbf{v} with respect to α_i ; and

$d'_{\delta\mathbf{u}}$, $a'_{\delta\mathbf{u}}$, and $l'_{\delta\mathbf{u}}$ are variations of the kinetic sesqui-linear form, structural sesqui-linear form, and load semi-linear form, respectively Kim, *et al.* (2002). A standard sensitivity calculation procedure is then obtained as follows. First, Equation (13) is solved for the velocity sensitivity $\frac{\partial\mathbf{v}}{\partial\alpha_i}$, and then the result is substituted into Equation (12) to obtain $\frac{\partial p}{\partial\alpha_i}$. It is seen that this procedure needs to be repeated for each design variable

used in the design problem. If the number of design variables is large, then the calculations will become extensive. However, if the *second adjoint variable vector* $\boldsymbol{\lambda}$ is defined as a solution of the following equation

$$j\omega d_{\mathbf{u}}(\bar{\boldsymbol{\lambda}}, \boldsymbol{\lambda}) + \kappa a_{\mathbf{u}}(\bar{\boldsymbol{\lambda}}, \boldsymbol{\lambda}) = b(\mathbf{x}_0; \bar{\boldsymbol{\lambda}}) + e(\mathbf{x}_0; A^{-1} \circ B(\bar{\boldsymbol{\lambda}})) \quad \forall \bar{\boldsymbol{\lambda}} \in Z \quad (14)$$

or equivalently in the discrete form as

$$(j\omega\mathbf{M} + \kappa\mathbf{K})\boldsymbol{\lambda}^* = \mathbf{L} \quad (15)$$

then Equation (12) can be simplified as

$$\frac{\partial\mathbf{v}}{\partial\alpha_i} = l'_{\theta\mathbf{u}}(\boldsymbol{\lambda}) - j\omega d'_{\theta\mathbf{u}}(\mathbf{v}, \boldsymbol{\lambda}) - \kappa a'_{\theta\mathbf{u}}(\mathbf{v}, \boldsymbol{\lambda}) \quad (16)$$

Note that both adjoint variable vectors, $\boldsymbol{\eta}$ defined in Equation (11) and $\boldsymbol{\lambda}$ defined in Equation (15), are independent of the design variable. And $\boldsymbol{\lambda}^*$ in Equation (15) is the complex conjugate of the adjoint variable $\boldsymbol{\lambda}$ due to the sesqui-linear form of $d_{\mathbf{u}}(\bullet, \bullet)$ and $a_{\mathbf{u}}(\bullet, \bullet)$ (Kim, *et al.*, 2002). Therefore, Equations (11) and (15) only need to be solved once regardless of how many design variables are used in the design problem. Solving Equations (11) and (15) are the major calculations in the sensitivity analysis process. When a large number of design variables are used, which is the usual case in a structural optimisation problem, significant savings can be obtained in terms of the computational cost. This is the major benefit from the use of the adjoint variables. More detailed discussions regarding this can be found in Kim, *et al.* (2002).

Also note that if the selected design variable only affects the properties of a substructure, a component in the structural system, then from Equation (16), we can have

$$\frac{\partial p}{\partial\alpha_i} = l'_{\theta\mathbf{u}}(\boldsymbol{\lambda}_e) - j\omega d'_{\theta\mathbf{u}}(\mathbf{v}_e, \boldsymbol{\lambda}_e) - \kappa a'_{\theta\mathbf{u}}(\mathbf{v}_e, \boldsymbol{\lambda}_e) \quad (17)$$

where \mathbf{v}_e and $\boldsymbol{\lambda}_e$ are components of the nodal velocity response and adjoint variable vectors with respect to the substructure, or component; and $d'_{\delta\mathbf{u}}$, $a'_{\delta\mathbf{u}}$, and $l'_{\delta\mathbf{u}}$ are variations of the energy forms with respect to the design change in the corresponding substructure or component. Furthermore, for a general structural or performance measure

which can be expressed by an integral form $\Psi = h(p(\mathbf{x}_0), \mathbf{u})$, its sensitivity can be evaluated by

$$\Psi = h_{\mathbf{u}} \delta \mathbf{u} + \ell^t_{\theta \mathbf{u}}(\lambda) - j \omega d^t_{\theta \mathbf{u}}(\mathbf{v}, \lambda) - \kappa a^t_{\theta \mathbf{u}}(\mathbf{v}, \lambda) \tag{18}$$

More detailed descriptions of the sensitivity of different performance measures and its calculation method can be found in Kim, et al. (2002).

Figure 4 illustrates the analysis and sensitivity analysis for the structural-acoustic system. Furthermore, Figure 5 summarises the actual computational procedure used for the design sensitivity analysis and optimisation (DSO), where DOT stands for Design Optimisation Tool.

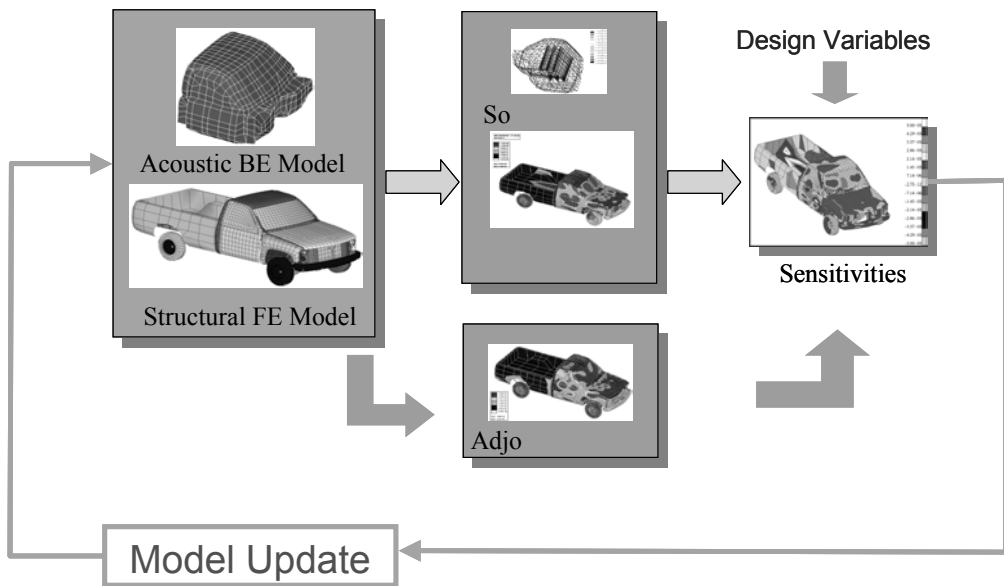


Figure 4 Analysis and sensitivity analysis of a structural-acoustic system.

3.3 Reduced order modelling (ROM) technique

The methodology of using characteristic constraint (CC) modes to generate a reduced order model for vibration analysis is now briefly described. First, the vehicle structure is divided into a set of substructures, which are also called component structures. For the truck considered in this study, the finite element (FE) model of the vehicle is partitioned into six substructures as shown in Figure 6. These six subsystems are referred to as: (1) cabin; (2) left door; (3) right door; (4) rail, which contains rails, front wheels, and bed; (5) front, which contains hood, wheelhouses, fenders, and radiator; (6) powertrain, which contains rear wheels and engine.

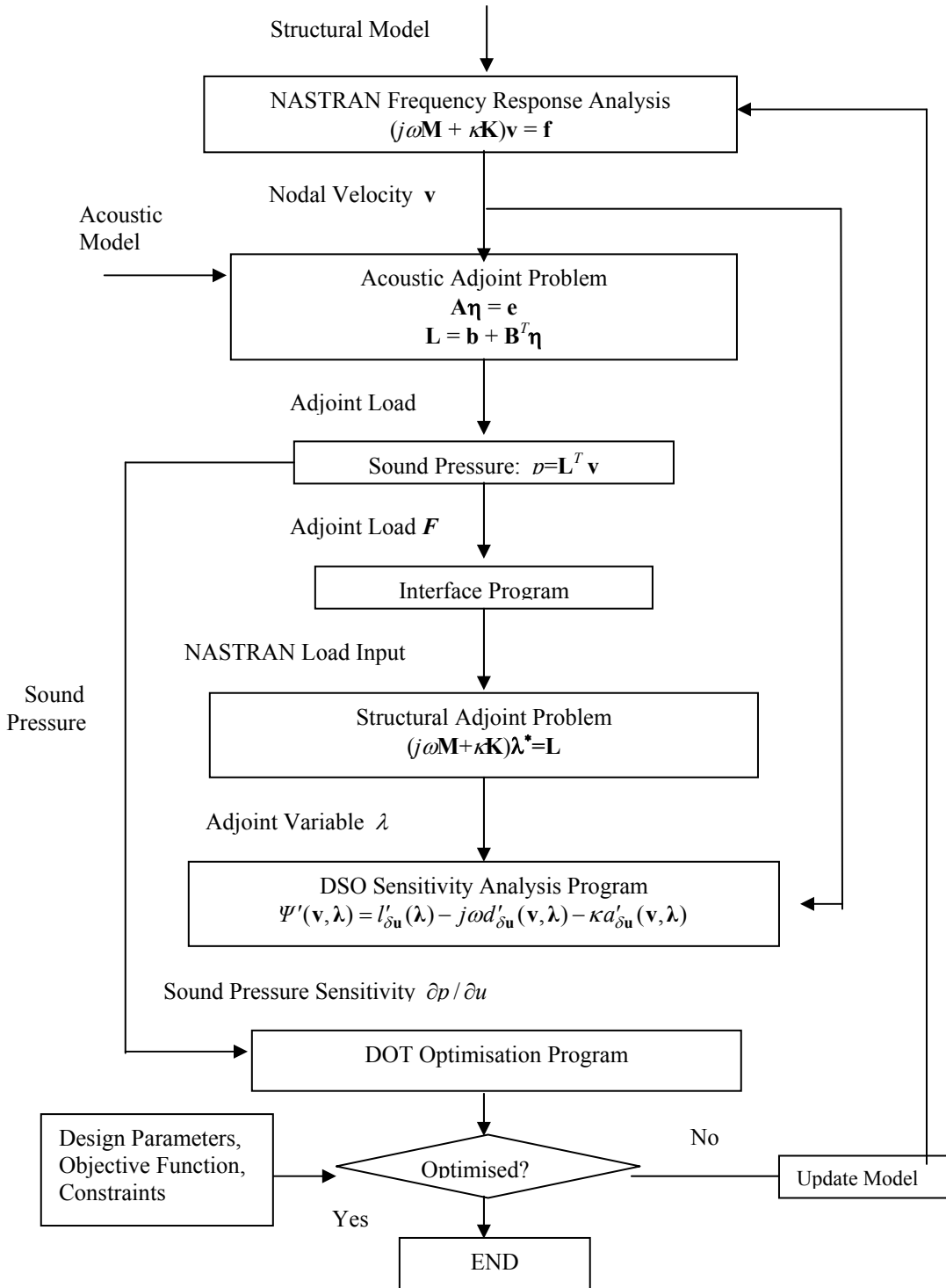


Figure 5 Computational procedure of design sensitivity analysis and optimisation.

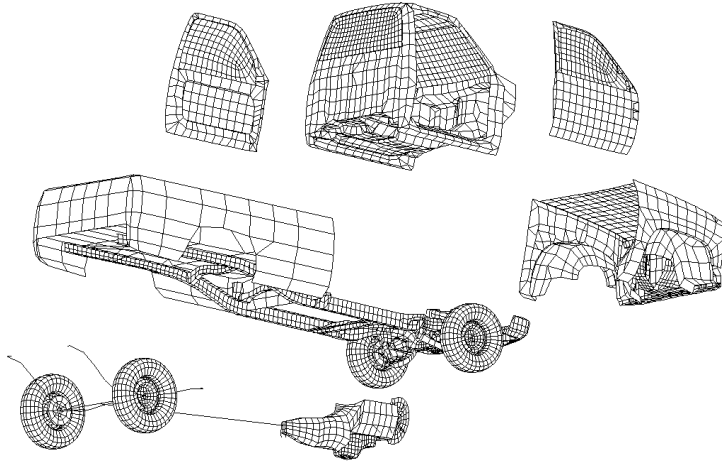


Figure 6 Substructuring of the FE model of the vehicle into 6 components.

Next, the mass and stiffness matrices from the component finite element models are partitioned into several sets of DOF: the interior DOF of each component, and the DOF in the interface between components. Then, the Craig-Bampton method (Craig, and Bampton, 1968) is used to generate a component mode synthesis (CMS) model of the global structure. This method utilises two sets of substructure modes: component normal modes, Φ_i^N , which are the modes of each component with the interface held fixed; and constraint modes, Φ_i^C , which are the static shapes induced by a unit displacement of each interface DOF with all other interface DOF held fixed.

Based on the constraint-mode and normal-mode coordinates, the velocity vector, \mathbf{v}^{CMS} , of the Craig-Bampton CMS model may be written as

$$\mathbf{v}^{CMS} = \left\{ \mathbf{v}^{C^T} \quad \mathbf{v}_1^{N^T} \quad \mathbf{v}_2^{N^T} \quad \dots \quad \mathbf{v}_{n^{SS}}^{N^T} \right\}^T \tag{19}$$

where the subscripts refer to individual substructures and n^{SS} is the number of substructures contained in the global structure. The corresponding CMS mass and stiffness matrices have the following form

$$\mathbf{M}^{CMS} = \begin{bmatrix} \mathbf{m}^{-C} & \mathbf{m}_1^{CN} & \mathbf{m}_2^{CN} & \dots & \mathbf{m}_{n^{SS}}^{CN} \\ \mathbf{m}_1^{CN^T} & \mathbf{m}_1^N & \mathbf{0} & \dots & \mathbf{0} \\ \mathbf{m}_2^{CN^T} & \mathbf{0} & \mathbf{m}_2^N & & \mathbf{0} \\ \vdots & \vdots & & \ddots & \vdots \\ \mathbf{m}_{n^{SS}}^{CN^T} & \mathbf{0} & \mathbf{0} & \dots & \mathbf{m}_{n^{SS}}^N \end{bmatrix} \tag{20}$$

$$\mathbf{K}^{CMS} = \begin{bmatrix} \bar{\mathbf{k}}^C & \mathbf{0} & \mathbf{0} & \cdots & \mathbf{0} \\ \mathbf{0} & \mathbf{k}_1^N & \mathbf{0} & \cdots & \mathbf{0} \\ \mathbf{0} & \mathbf{0} & \mathbf{k}_2^N & & \mathbf{0} \\ \vdots & \vdots & & \ddots & \vdots \\ \mathbf{0} & \mathbf{0} & \mathbf{0} & \cdots & \mathbf{k}_{n,ss}^N \end{bmatrix} \quad (21)$$

The component modal matrices, \mathbf{m}_i^N and \mathbf{k}_i^N , are diagonal, and their sizes depend on the number of modes selected for the frequency range of interest. However, if the standard Craig-Bampton method is used, there is necessarily one constraint mode for each DOF in the interface region of the finite element model, and thus the size of $\bar{\mathbf{m}}^C$ and $\bar{\mathbf{k}}^C$ is equal to the number of interface DOF. Therefore, while the component partitions are, in general, greatly reduced relative to the parent finite element model, there is no reduction for the interface DOF. For large-scale models of vehicle structures, the size of the CMS model may be dominated by the interface DOF.

To generate a low-order model, a secondary modal analysis is performed on the constraint-mode DOF:

$$\bar{\mathbf{k}}^C \psi_n = \lambda_n \bar{\mathbf{m}}^C \psi_n \quad (22)$$

These eigenvectors, ψ_n , may be expressed in finite element coordinates for component structure i using the following transformation

$$\Phi_i^{CC} = \Phi_i^C \beta_i^C \Psi \quad (23)$$

where $\Psi = [\psi_1 \ \psi_2 \ \cdots \ \psi_{n,cc}]$ is a selected set of the interface eigenvectors with n^{CC} indicating the number of the selected eigenvectors, and β_i^C is the matrix that maps the global interface DOF, \mathbf{v}^C , to the local DOF, \mathbf{v}_i^C . The vectors Φ_i^{CC} are referred to as the characteristic constraint (CC) modes, since they are eigenvector-based linear combinations of constraint modes that provide a set of characteristic displacement shapes for the interface (Castanier, *et al.*, 2001).

The CMS model can now be transformed to a reduced order model (ROM) by selecting a truncated set of CC modes for the frequency range of interest, and then using these vectors to project the CMS matrices onto the reduced basis. The velocity vector is now of the form:

$$\mathbf{v}^{ROM} = \left\{ \mathbf{v}^{CC^T} \ \mathbf{v}_1^{N^T} \ \mathbf{v}_2^{N^T} \ \cdots \ \mathbf{v}_{n,ss}^{N^T} \right\}^T \quad (24)$$

where the superscript CC indicates the partition associated with the CC modes. The reduced-order CMS model of Equation (7) can be expressed by

$$(j\omega\mathbf{M}^{ROM} + \kappa\mathbf{K}^{ROM})\mathbf{v}^{ROM} = \mathbf{f}^{ROM} \quad (25)$$

The mass matrix, \mathbf{M}^{ROM} , the stiffness matrix, \mathbf{K}^{ROM} , and the applied force vector, \mathbf{f}^{ROM} , can be explicitly written as

$$\mathbf{M}^{ROM} = \begin{bmatrix} \overline{\mathbf{m}}^{CC} & \overline{\mathbf{m}}^{CN} & \overline{\mathbf{m}}^{CN} & \cdots & \overline{\mathbf{m}}^{CN}_{n^{SS}} \\ \overline{\mathbf{m}}_1^{CN^T} & \mathbf{m}_1^N & \mathbf{0} & \cdots & \mathbf{0} \\ \overline{\mathbf{m}}_2^{CN^T} & \mathbf{0} & \mathbf{m}_2^N & & \mathbf{0} \\ \vdots & \vdots & & \ddots & \vdots \\ \overline{\mathbf{m}}_{n^{SS}}^{CN^T} & \mathbf{0} & \mathbf{0} & \cdots & \mathbf{m}_{n^{SS}}^N \end{bmatrix} \quad (26)$$

$$\mathbf{K}^{ROM} = \begin{bmatrix} \overline{\mathbf{k}}^{CC} & \mathbf{0} & \mathbf{0} & \cdots & \mathbf{0} \\ \mathbf{0} & \mathbf{k}_1^N & \mathbf{0} & \cdots & \mathbf{0} \\ \mathbf{0} & \mathbf{0} & \mathbf{k}_2^N & & \mathbf{0} \\ \vdots & \vdots & & \ddots & \vdots \\ \mathbf{0} & \mathbf{0} & \mathbf{0} & \cdots & \mathbf{k}_{n^{SS}}^N \end{bmatrix} \quad (27)$$

$$\mathbf{f}^{ROM} = \left[\overline{\mathbf{f}}^{CC^T} \quad \mathbf{f}_1^{N^T} \quad \mathbf{f}_2^{N^T} \quad \cdots \quad \mathbf{f}_{n^{SS}}^{N^T} \right]^T \quad (28)$$

where

$$\overline{\mathbf{m}}^{CC} = \Psi^T \overline{\mathbf{m}}^C \Psi \quad \overline{\mathbf{k}}^{CC} = \Psi^T \overline{\mathbf{k}}^C \Psi \quad \overline{\mathbf{m}}_i^{CN} = \Psi^T \beta_i^{C^T} \mathbf{m}_i^{CN} \quad \overline{\mathbf{f}}^{CC} = \Psi^T \overline{\mathbf{f}}^C \quad (29)$$

Now, every matrix partition has been reduced by some form of modal analysis.

It should be noted that the ROM can be used not only to calculate the vibration response, but also the vibration energy that is transmitted between component structures, which is referred to as the power flow. Using power flow analysis, the energy levels of the substructures can be calculated, and the paths of vibration transmission from the source to key response points can be identified. This information can also be used for design sensitivity analysis and optimisation.

Since the power is transmitted between substructures through the interface motion, the power flow is described only by the CC modes in this ROM. However, in order to perform efficient computations, the power flow may be projected onto the global modes of the ROM. First, an eigen-analysis is performed

$$\mathbf{K}^{ROM} \mathbf{\Gamma} = \mathbf{M}^{ROM} \mathbf{\Gamma} \mathbf{\Lambda} \quad (30)$$

where the eigenmatrix can be partitioned as

$$\mathbf{\Gamma} = \begin{bmatrix} \boldsymbol{\gamma}^{CC^T} & \boldsymbol{\gamma}_1^{N^T} & \boldsymbol{\gamma}_2^{N^T} & \cdots & \boldsymbol{\gamma}_{n^{ss}}^{N^T} \end{bmatrix}^T \quad (31)$$

Then Equation (25) can be transformed to

$$\left(j\omega \overline{\mathbf{M}} + \kappa \overline{\mathbf{K}} \right) \overline{\mathbf{v}} = \overline{\mathbf{f}} \quad (32)$$

where $\overline{\mathbf{M}} = \mathbf{\Gamma}^T \mathbf{M}^{ROM} \mathbf{\Gamma}$, $\overline{\mathbf{K}} = \mathbf{\Gamma}^T \mathbf{K}^{ROM} \mathbf{\Gamma}$, $\overline{\mathbf{f}} = \mathbf{\Gamma}^T \mathbf{f}^{ROM}$.

For time-harmonic excitation, the power flow can be formulated in terms of $\overline{\mathbf{v}}$

$$\Pi_i(\omega) = \frac{1}{2} \text{Re} \left[\overline{\mathbf{f}}_i^* \overline{\mathbf{v}} \right] - \frac{1}{2} \overline{\mathbf{v}}^* \overline{\mathbf{C}}_i \overline{\mathbf{v}} \quad (33)$$

where $\overline{\mathbf{C}}_i$ is the damping of the substructure i projected onto the global modes of the ROM

$$\overline{\mathbf{C}}_i = \boldsymbol{\gamma}^{CC^T} \text{Re} \left[\mathbf{z}_i^{CC} \right] \boldsymbol{\gamma}^{CC} + \boldsymbol{\gamma}_i^{N^T} \text{Re} \left[\mathbf{z}_i^N \right] \boldsymbol{\gamma}_i^N \quad (34)$$

where \mathbf{z}_i^{CC} is the impedance matrix of substructure i associated with CC modes, and \mathbf{z}_i^N is the impedance matrix of substructure i associated with component modes. In addition, $\overline{\mathbf{f}}_i$ is given by

$$\overline{\mathbf{f}}_i = \boldsymbol{\gamma}_i^{N^T} \mathbf{f}_i^N + \boldsymbol{\gamma}^{CC^T} \mathbf{f}_i^{CC} \quad (35)$$

where \mathbf{f}_i^{CC} is the applied force for the CC-mode coordinates of substructure i .

3.4 Energy boundary element analysis (EBEA)

In this subsection, an energy boundary element analysis (EBEA) formulation is presented for computing high-frequency acoustic radiation from incoherent intensity boundary conditions defined on the surface of the radiator. The frequency-averaged acoustic energy density and intensity constitute the primary variables for EBEA. The corresponding integral formulation is derived based on the governing integral equation of the conventional boundary element method (BEM) (Chen, and Schweikert, 1963; Brebbia, *et al.*, 1984).

The basic assumption in deriving the EBEA formulation is that the infinitesimal energy sources on each element are incoherent among different elements. This assumption is in line with the existing high-frequency statistical energy analysis (SEA) (Lyon, 1975) and energy finite element analysis (EFEA) (Vlahopoulos, *et al.*, 1999; Zhang, *et al.*, 2002; Zhang, *et al.*, 2001) formulations, and it is also necessary in order to

potentially utilise the incoherent acoustic power computed by the EFEA analysis on the outer part of a structure as a boundary condition for predicting the radiated acoustic field.

The EBFA numerical formulation is developed by placing a continuous distribution of incoherent infinitesimal energy sources on the surface of the radiator. The acoustic power on each element comprises the prescribed boundary conditions of the EBFA. The EBFA is employed in this work for computing the high frequency acoustic field around the vehicle. This information can be used in the future as excitation for an airborne interior noise analysis (Wang, *et al.*, 1999).

The EBFA formulation is developed from the integral formulas for the acoustic pressure or velocity of the conventional boundary element method. First, the acoustic energy density and intensity at a field point Y is time-averaged over a period and expressed in terms of the acoustic velocity and the acoustic pressure as (Pierce, 1981):

$$\langle e_Y \rangle = \frac{1}{4} \left(\rho \hat{\mathbf{v}}_Y \cdot \hat{\mathbf{v}}_Y^* + \frac{1}{\rho c^2} \hat{p}_Y \hat{p}_Y^* \right) \quad (36)$$

$$\langle \mathbf{I}_Y \rangle = \frac{1}{2} \text{Re} \left(\hat{p}_Y \hat{\mathbf{v}}_Y^* \right) \quad (37)$$

where ρ is the density of the acoustic medium, subscript ‘Y’ indicates a quantity associated with a field point Y, c is the speed of the sound in the medium, $\hat{\mathbf{v}}$ and \hat{p} are the acoustic velocity and the acoustic pressure, respectively, $\langle \rangle$ indicates time averaging over a period (i.e., $\langle A \rangle = \left(\frac{1}{T} \right) \int_t^{t+T} A(\tau) d\tau$), and symbol $\hat{}$ indicates complex quantities. In order to develop the primary variables of EBFA, the ensemble-averaging operator $E[\cdot]$ is applied on the equations for $\langle e_Y \rangle$ and $\langle \mathbf{I}_Y \rangle$, yielding:

$$\tilde{e}_Y = E[\langle e_Y \rangle] = \frac{1}{4} \left(\rho E[\hat{\mathbf{v}}_Y \cdot \hat{\mathbf{v}}_Y^*] + \frac{1}{\rho c^2} E[\hat{p}_Y \hat{p}_Y^*] \right) \quad (38)$$

and

$$\tilde{\mathbf{I}}_Y = E[\langle \mathbf{I}_Y \rangle] = \frac{1}{2} \text{Re} \left(E[\hat{p}_Y \hat{\mathbf{v}}_Y^*] \right) \quad (39)$$

Since the ensemble averaging in the high-frequency methods is considered equivalent to frequency averaging (Lyon, 1975; Vlahopoulos, and Zhao, 2001; Keane, 1993; Wester, and Mace, 1996; Andrew, and Kirlin, 2000), \tilde{e}_Y and $\tilde{\mathbf{I}}_Y$ are equivalent to the time-averaged (over a period) and frequency-averaged (over 1/3 octave band) energy density and intensity at a field point Y.

In the conventional indirect boundary integral method, the acoustic pressure at any field point Y exterior to the structure is expressed as (Chen, and Schweikert, 1963; Brebbia, *et al.*, 1984)

$$\hat{p}_Y = \int_S A(P) g(P, Y) dS \quad (40)$$

where S is the surface of the structure, P denotes the point located on the surface S , $A(P)$ is the complex source strength amplitude at P , $g(P, Y) = \frac{e^{-ikr}}{4\pi r}$ is the Green's function for the three-dimensional infinite domain, r is the distance between points P and Y , and k is the wavenumber.

The acoustic velocity vector can be obtained from the acoustic pressure

$$\hat{v}_Y = -\frac{1}{i\omega\rho} \nabla \hat{p}_Y = -\frac{1}{i\omega\rho} \int_S A \nabla g(P, Y) dS, \quad (41)$$

where:

$$\nabla g(P, Y) = -\frac{1}{4\pi r^2} (1 + ikr) e^{-ikr} \mathbf{E}_r, \quad (42)$$

\mathbf{E} denotes the unit vector from P to Y .

Equations (40) and (41) are employed for developing expressions for the ensemble-averaged quantities $E[\hat{p}_Y \hat{p}_Y^*]$, $E[\hat{v}_Y \cdot \hat{v}_Y^*]$ and $E[\hat{p}_Y \hat{v}_Y^*]$. The latter expressions are introduced in Equations (38) and (39) in order to develop the equations for the primary variables of the EBEA formulation. The acoustic pressure square is calculated as:

$$\begin{aligned} \hat{p}_Y \hat{p}_Y^* &= \int_S A(P') g(P', Y) dS \cdot \int_S A^*(P'') g^*(P'', Y) dS \\ &= \int_S \int_S A(P') A^*(P'') g(P', Y) g^*(P'', Y) dS' dS'' \end{aligned} \quad (43)$$

For incoherent sources, $E[A(P') A^*(P'')]$ is non-zero only for $P' = P''$ (Andrew, and Kirilin, 2000; Li, and Pascal, 1998). Thus, by applying the operator $E[\cdot]$ to Equation (43) results in:

$$E[\hat{p}_Y \hat{p}_Y^*] = \int_S \int_S E[A(P') A^*(P'')] g(P', Y) g^*(P'', Y) dS' dS'' = \mu \int_S |A(P)|^2 |g(P, Y)|^2 dS \quad (44)$$

In Equation (44) the double integral is reduced to a single integral due to the zero cross terms in $E[A(P') A^*(P'')]$. The constant μ retains the proper units during the reduction from a double to a single integral. In the case of Equation (44), μ is equal to $\int_S dS$.

Following a similar process for $E[\hat{v}_Y \cdot \hat{v}_Y^*]$ and $E[\hat{p}_Y \hat{v}_Y^*]$ results in:

$$E[\hat{\mathbf{v}}_Y \hat{\mathbf{v}}_Y^*] = \frac{\mu}{\omega^2 \rho^2} \int_S |A(\mathbf{P})|^2 |\nabla g(\mathbf{P}, \mathbf{Y})|^2 dS \quad (45)$$

and

$$E[\hat{p}_Y \hat{\mathbf{v}}_Y^*] = \frac{\mu}{i\omega\rho} \int_S |A(\mathbf{P})|^2 g(\mathbf{P}, \mathbf{Y}) \nabla g^*(\mathbf{P}, \mathbf{Y}) dS \quad (46)$$

Substituting Equations (44) and (45) into Equation (38), results in

$$\tilde{e}_Y = \frac{\mu}{\rho^2 \omega^2} \int_S |A(\mathbf{P})|^2 \left(\frac{\rho}{64\pi^2 r^4} + \frac{k^2 \rho}{32\pi^2 r^2} \right) dS \quad (47)$$

Similarly, substituting Equation (46) into Equation (39), results in

$$\tilde{\mathbf{I}}_Y = \frac{\mu}{\rho^2 \omega^2} \int_S |A(\mathbf{P})|^2 \frac{k^2 \rho c}{32\pi^2 r^2} \mathbf{E}_r dS \quad (48)$$

In Equations (47) and (48), the term $\frac{\mu}{\rho^2 \omega^2}$ is a frequency-dependent term. The strength density of the energy source or sink can be defined as the product of this frequency-dependent term and $|A(\mathbf{P})|^2$

$$\sigma(\mathbf{P}) = \frac{\mu}{\rho^2 \omega^2} |A(\mathbf{P})|^2 \quad (49)$$

where σ denotes the strength density of the energy source. Thus, Equations (47) and (48) can be written in their final form as:

$$\tilde{e}_Y = \int_S \sigma(\mathbf{P}) \left(\frac{\rho}{64\pi^2 r^4} + \frac{k^2 \rho}{32\pi^2 r^2} \right) dS \quad (50)$$

and

$$\tilde{\mathbf{I}}_Y = \int_S \sigma(\mathbf{P}) \frac{k^2 \rho c}{32\pi^2 r^2} \mathbf{E}_r dS \quad (51)$$

Equations (50) and (51) constitute the basic integral equations of the EBEA formulation. The acoustic energy density and intensity at any field point exterior to the structure can be determined by Equations (50) and (51), respectively. Comparing to the conventional indirect boundary integral method, the Green's functions for the time and frequency averaged acoustic energy density and intensity in the free field can be obtained from above two integrals, respectively

$$G(\mathbf{P}, \mathbf{Y}) = \frac{\rho}{64\pi^2 r^4} + \frac{k^2 \rho}{32\pi^2 r^2} \quad (52)$$

$$\mathbf{H}(\mathbf{P}, \mathbf{Y}) = \frac{k^2 \rho c}{32\pi^2 r^2} \mathbf{E}_r \quad (53)$$

To develop a numerical solution, the surface S of the radiator (Figure 7) is divided into n quadrilateral or triangular elements. Incoherent infinitesimal energy sources or sinks are distributed on every element. In this work, the source strength density σ_j ($j=1, 2, \dots, n$) on each element is considered to be constant. Equations (50) and (51) can be rewritten in the discrete form as:

$$\tilde{e}_Y = \sum_{j=1}^n \left(\sigma_j \int_{S_j} G(\xi, \mathbf{Y}) dS \right) \quad (54)$$

$$\tilde{\mathbf{I}}_Y = \sum_{j=1}^n \left(\sigma_j \int_{S_j} \mathbf{H}(\xi, \mathbf{Y}) dS \right) \quad (55)$$

where S_j indicates the surface of element j as shown in Figure 7, ξ is an arbitrary point on the element j . On each element, the source strength density σ_j is constant and can be factored outside of the integral. In order to develop the numerical system of equations that will allow to compute the values of the sources and sinks σ_j over the model, the field point \mathbf{Y} is placed on an element q on the outer surface of the radiator and Equation (55) provides the integral equation for the intensity $\tilde{\mathbf{I}}_Y$ on the element q . In order to avoid the singular integration within the element q in Equation (55), the definition of the averaged acoustic power radiated by element q itself is employed (Wang, *et al.*, 2002).

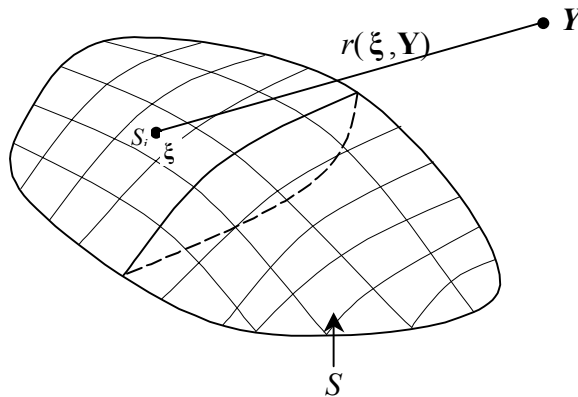


Figure 7 Surface of an EBEA model divided into n quadrilaterals (or triangles).

Since the radiated acoustic power from each element comprises the prescribed boundary condition, the time and frequency averaged intensity on an element integrated over the area of the element must result into the prescribed radiated acoustic power:

$$\int_{s_i} \tilde{\mathbf{I}}_Y \cdot \mathbf{n}_i dS = \bar{P}_i, \quad i=1,2,\dots,n \quad (56)$$

where \bar{P}_i is the prescribed boundary condition on element i , \mathbf{n}_i is the normal (outward of the structure) vector of the element i . Substituting Equation (55) in the above equation results in the governing equation of EBEA

$$K_{ij} \sigma_j = \bar{P}_i, \quad i=1,2,\dots,n, \quad j=1,2,\dots,n \quad (57)$$

For any set of prescribed boundary conditions, the values of the acoustic energy source strength density on each element can be obtained by solving Equation (57). Then by employing Equations (54) and (55), the time and frequency averaged acoustic energy density and intensity can be determined at any field point in the acoustic medium.

4 Conclusions

In this paper, several new methodologies have been presented for the design and virtual prototyping of advanced structures. An improved topology optimisation technique can lay out novel, conceptually advanced designs for vehicle structures or substructures to achieve the goals of lightweight and high-performance in next-generation ground vehicles. A ‘sizing’ design optimisation process can then be used to determine more detailed design changes of the vibration-noise system in dealing with a complex vehicle structure. The new FEA-BEA sensitivity analysis method with sequential adjoint variable vectors can significantly improve computational efficiency of the sensitivity analysis and thus the optimisation process. A component-based modelling technique can greatly reduce the size of the vehicle vibration models, and it can also be used to predict the power flow between substructures as well as the effect of parameter uncertainties on the system response. Finally, an energy boundary element analysis method can be used for efficient and accurate high-frequency noise analysis, which extends the capability for predicting the acoustic field around the vehicle due to various sources. In the companion paper, these methodologies will be applied to a case study of a pick-up truck.

5 Acknowledgements

This research is supported by the Automotive Research Center, which is sponsored by the US Army TARDEC under contract DAAE07-98-3-0022.

References

- Andrew, R.K. and Kirlin, R.L. (2000) 'A broadband maximum likelihood imager for a class of extended space-time separable sources', *IEEE Transactions on Signal Processing*, Vol. 48, pp. 1287-1294.
- Bendsøe, M. P. and Kikuchi, N. (1988) 'Generating optimal topologies in structural design using a homogenization method', *Comput. Methods. Mech. Energ.*, Vol. 71, pp. 197-24.
- Berke, L. and Khot, N.S. (1987) 'Structural optimization using optimality criteria', *Computer Aided Optimal Design: Structural and Mechanical Systems* (Mota Soares, C.A., Editor), Springer-Verlag, pp. 271-311.
- Brebbia, C.A., Telles, J.C. and Wrobel, L.C. (1984) *Boundary Element Techniques*, Springer-Verlag, Berlin.
- Castanier, M.P., Tan, Y.C. and Pierre, C. (2001) 'Characteristic constraint modes for component mode synthesis', *AIAA Journal*, Vol. 39, pp. 1182-1187
- Chen, L.H. and Schweikert, D.G. (1963) 'Sound radiation from an arbitrary body', *Journal of the Acoustical Society of America*, Vol. 35, pp. 1626-1632.
- Choi, K.K., and Lee, J.H. (1992) 'Sizing design sensitivity analysis of dynamic frequency response of vibrating structures', *ASME Journal of Mechanical Design*, **114**, pp. 166-173.
- Choi, K.K., Shim, I. and Wang, S. (1997) 'Design sensitivity analysis of structure-induced noise and vibration', *Journal of Vibration and Acoustics*, Vol. 119, pp. 173-179.
- Ciskowski, R.D. and Brebbia, C.A. (1991) *Boundary Elements in Acoustics*, Elsevier Applied Science, New York, NY.
- Craig, R.R. and Bampton, M.C.C. (1968) 'Coupling of substructures for dynamic analyses', *AIAA Journal*, Vol. 6, pp. 1313-1319.
- D. Wang, Goetchius, G.M. and Onsay, T. (1999) 'Validation of a SEA model for a minivan: use of ideal air- and structure-borne sources', SAE Noise and Vibration Conference, Traverse City, May 1999, SAE Paper 1999-01-1697, pp. 381-388.
- Fecker, M., Ananthasuresh, G.K., Kikuchi, N. and Kota, S. (1997) 'Topological synthesis of compliant mechanisms using multi-criteria optimization', *Journal of Mechanical Design*, ASME Transactions, Vol. 119, No. 2, pp. 238-245.
- Fleury, C. (1987) 'Efficient approximation concepts using second order information', *Int. J. Numerical Methods in Engineering*, Vol. 28, pp. 2041-2058.
- Fleury, C. and Braibant, V. (1986) 'Structural optimization: a new dual method using mixed variables', *Int. J. Numerical Methods in Engineering*, Vol. 23, pp. 409-428.
- Hong, S.B. and Vlahopoulos, N. (2003) 'Hybrid finite element formulation for Analyzing Systems of Beams and Plates in the Mid-Frequency Range', SAE noise and vibration conference', Traverse City, May 2003, SAE Paper 2003-01-1610.
- Keane, A.J. (1993) 'A note on modal summations and averaging methods as applied to statistical energy analysis (S.E.A.)', *Journal of Sound and Vibration*, Vol. 164, pp. 143-156.
- Kikuchi, N., Nishiwaki, S., Fonseca, J. O. and Silva, E.C.N. (1998) 'Design optimization method for compliant mechanisms and material microstructure', *Comput. Methods. Mech. Energ.*, Vol. 151, pp. 401-417.
- Kim, N.H., Choi, K.K., Dong J., Pierre C., Vlahopoulos N., Ma, Z.-D. and Castanier, M. (2001) 'A sequential adjoint variable method in design sensitivity analysis of NVH problems', Symposium on Advanced Techniques for Structural Acoustics, *Proceedings of ASME 2001 International Mechanical Engineering Congress & Exposition*, November 11-16, 2001, New York, New York, Volume 3, IMECE2001/NCA, 1-10.

- Kim, N.H., Dong J., Choi, K.K., Vlahopoulos, N., Ma, Z.-D., Castanier, M. and Pierre, C. (2002) 'Design sensitivity analysis for a sequential structural-acoustic problem', *Journal of Sound and Vibration*, Vol. 263, No. 3, pp. 569-591.
- Li, J. and Pascal, J. (1998) 'Energy fields of partially coherent sources', *Journal of the Acoustical Society of America*, Vol. 103, pp. 962-972.
- Lyon, R. (1975) *Statistical Energy Analysis of Dynamical Systems: Theory and Application*, MIT Press, Cambridge, MA.
- Ma, Z.-D. and Kikuchi, N. (1995) 'A new method of the sequential approximate optimization', *Engineering Optimization*, Vol. 25, pp. 231-253.
- Ma, Z.-D., Kikuchi, N. and Cheng, H.-C. (1995) 'Topological design for vibrating structures', *Comput. Methods. Mech. Energ.*, Vol. 121, pp. 259-280.
- Ma, Z.-D., Kikuchi, N. and Hagiwara, I., 1993, 'Structural Topology and Shape Optimization for a Frequency Response Problem', *Computational Mechanics*, Vol. 13, No. 3, pp. 157-174.
- Ma, Z.-D., Kikuchi, N., Cheng, H.-C. and Hagiwara, I. (1995) 'Topological optimization technique for free vibration problems', *ASME Journal of Applied Mechanics*, Vol. 62, pp. 200-207.
- Ma, Z.-D., Kikuchi, N., Cheng, H.-C. and Hagiwara, I., 1994, 'Structural Design for Obtaining Desired Frequencies by Using the Topology and Shape Optimization Method', *Computing System in Engineering*, Vol. 5, No. 1, pp. 77-89.
- Ma, Z.-D., Kikuchi, N., Pierre, C. and Raju, B. (2002) 'Multi-domain topology optimization for vehicle substructure design', *Proceedings of 2002 ASME International Mechanical Engineering Congress and Exposition*, New Orleans, Louisiana, November 17-22, 2002.
- Ma, Z.-D., Kikuchi, N., Pierre, C. and Raju, B. (2003) 'Substructure design using a multi-domain multi-step topology optimization approach', 2003 SAE World Congress, SAE Paper 03B-125, pp. 1-9.
- Nishiwaki, S., Frecker, M., Min, S. J. and Kikuchi, N. (1998) 'Topology optimization of compliant mechanisms using the homogenization method', *Int. J. Numerical Methods in Engineering*, Vol. 42, pp. 535-559.
- Pierce, A.D. (1981) *Acoustics: An Introduction to its Physical Principles and Applications*, McGraw Hill Press, New York.
- Pierre, C., Vlahopoulos, N., Ma, Z.-D., Castanier, M.P., Lee, S.-Y., Wang, A., Choi, K.K., Kim, N.H. and Dong, J. (2004) 'Advanced structure methodologies for next-generation ground vehicles, Part 2: A case study', *International Journal of Heavy Vehicle Systems*, Vol. 11, Nos. 3/4, pp.xxx-xxx.
- Svanberg, K. (1987) 'The method of moving Asymptotes--a new method for structural optimization', *Int. J. Numerical Methods in Engineering*, Vol. 24, pp. 359-373.
- Vlahopoulos, N. and Zhao, X. (1999) 'Basic development of a hybrid finite element method for mid-frequency computations of structural vibrations', *AIAA Journal*, Vol. 37, No. 11, pp. 1495-1505.
- Vlahopoulos, N. and Zhao, X. (2001) 'An investigation of power flow in the mid-frequency range for systems of co-linear beams based on a hybrid finite element formulation', *Journal of Sound and Vibration*, Vol. 242, pp. 445-473.
- Vlahopoulos, N., Luis, O.G. and Christopher, M. (1999) 'Numerical implementation, validation, and marine applications of an energy finite element formulation', *Journal of Ship Research* Vol. 43, pp. 143-156.
- Wang, A., Vlahopoulos, N. and Wu K. (2002) 'An energy boundary element formulation for sound radiation at high frequency', *The International Congress and Exposition on Noise Control Engineering*, ASME Paper No. 2002-405.

- Wang, H., Ma, Z.-D., Kikuchi, N., Pierre, C. and Raju, B. (2003) 'Numerical and experimental verification of optimum design obtained from topology optimization', 2003 SAE World Congress, SAE Paper 03B-121, pp. 1-8.
- Wester, E.C.N. and Mace, B.R. (1996) 'Statistical energy analysis of two edge-coupled rectangular plates: ensemble averages', *Journal of Sound and Vibration*, Vol. 193, pp. 793-822.
- Zhang, W., Wang, A. and Vlahopoulos, N. (2001) 'Validation of the EFEA method through correlation with conventional FEA and SEA results', *Proceedings of the 2001 SAE Noise and Vibration Conference*, SAE paper 2001-01-1618.
- Zhang, W., Wang, A. and Vlahopoulos, N. (2002) 'An alternative energy finite element formulation based on incoherent orthogonal waves and its validation for marine structures', *Finite Elements in Analysis and Design*, Vol. 38, pp. 1095-1113.
- Zhao, X. and Vlahopoulos, N. (2000) 'Hybrid finite element formulation for mid-frequency analysis of systems with excitation applied on short members', *Journal of Sound and Vibration*, Vol. 237, No. 2, pp. 181-202.